

Supplementary information

**Nitroxyl Radical-Containing Flexible Porous Coordination Polymer for Controllable
Size-Selective Aerobic Oxidation of Alcohols**

Ping Wang, Ziqian Xue, Otake Kenichi* and Susumu Kitagawa*

Institute for Integrated Cell-Material Sciences, Kyoto University Institute for Advanced Study,
Kyoto University, Yoshida Ushinomiya-cho, Sakyo-ku, Kyoto 606-8501, Japan

Materials and methods

All chemicals were used as received without any further purification. 2,5-Dibromobenzoic acid, 4-pyridine boronic acid, and oxalyl chloride were purchased from Tokyo Chemical Industries (TCI), Wako, and Nacalai Tesque, respectively. 4-Amino-2,2,6,6-tetramethylpiperidine 1-oxyl and 4-(methoxycarbonyl) phenylboronic acid were purchased from BLD Pharmatech Ltd. Acetonitrile-*d*3 was purchased from Wako, and other deuterated solvents for nuclear magnetic resonance (NMR) spectroscopy were purchased from Cambridge Isotope Laboratories. All solvent and other materials were purchased from either Nacalai Tesque or Wako Pure Chemicals.

¹H-NMR spectra were measured at 25°C on Bruker models Ultrashild 500 Plus NMR spectrometer, where chemical shifts (δ in ppm) were determined with a residual proton of the solvent standard. Thermogravimetric analyses (TGA) were performed on a Rigaku model Thermo plus EVO with a heating rate of 5 °C/min under N₂ flow. Powder X-ray diffraction (PXRD) data were recorded on a Rigaku SmartLab X-ray diffractometer using Cu-K α radiation ($\lambda = 1.54178$ Å) by depositing powder on a glass substrate, from $2\theta = 5^\circ$ up to 40° with 0.02° increment. Using cryostatic temperature controllers, gas and vapor adsorption experiments were carried out on the BELSORP MAX adsorption instrument (MicrotracBEL, Japan). The electron paramagnetic resonance (EPR) spectra were recorded for the polycrystalline PCP at room temperature with a JEOL JES-TE 200 X-band ESR spectrometer. Single crystals were picked with paraton oil on the glass fiber tip and mounted on a Rigaku XtaLAB P200 diffractometer equipped with Doctors PILATUS 200 K detector and Mo-K α radiation ($\lambda = 0.71073$ Å) whose temperature was controlled by liquid nitrogen. Synchrotron single-crystal X-ray diffraction measurement was performed using a Rigaku 1/4-chi goniometer with a PILATUS3 X CdTe 1M photon-counting detector installed in the BL02B1 beamline of SPring-8 ($\lambda = 0.41280$ Å) under cold N₂ gas flow. Crystal structures were solved by intrinsic phase methods of SHELXT (ver. 2018) and refined by full-matrix least-squares cycles in SHELXL (ver. 2018) using Yadokari-XG software package. All non-hydrogen atoms were refined using anisotropic thermal parameters. The electron densities corresponding to the disordered solvent molecules were flattened using PLATON SQUEEZE program. Crystallographic data for the crystal structures in CIF format has been deposited in the Cambridge Crystallographic Data Centre (CCDC) under deposition numbers listed in Table S1. The data can be obtained free of charge via www.ccdc.cam.ac.uk/data_request/cif (or from the Cambridge Crystallographic Data Centre, 12 Union Road, Cambridge CB2 1EZ, U.K.)

Catalytic reaction

Aerobic oxidation reaction catalyzed by DT-PCP.

Guest-free microcrystalline DT-PCP powder (5 mg, 5 mol% equiv.) was added into a Schlenk tube containing the reaction solvents, either CD₃CN, acetone-*d*₆, or DCM (1.5 mL). The alcohol substrate (0.1 mmol) and tert-butyl nitrite (0.02 mmol, 2.06 mg) were also added to the tube. The tube was then sealed and connected to an O₂ balloon. The reaction mixture was stirred at 35°C for 24 to 48 h. The alcohol conversion was confirmed by ¹H NMR analysis of the reaction mixture supernatant solution.

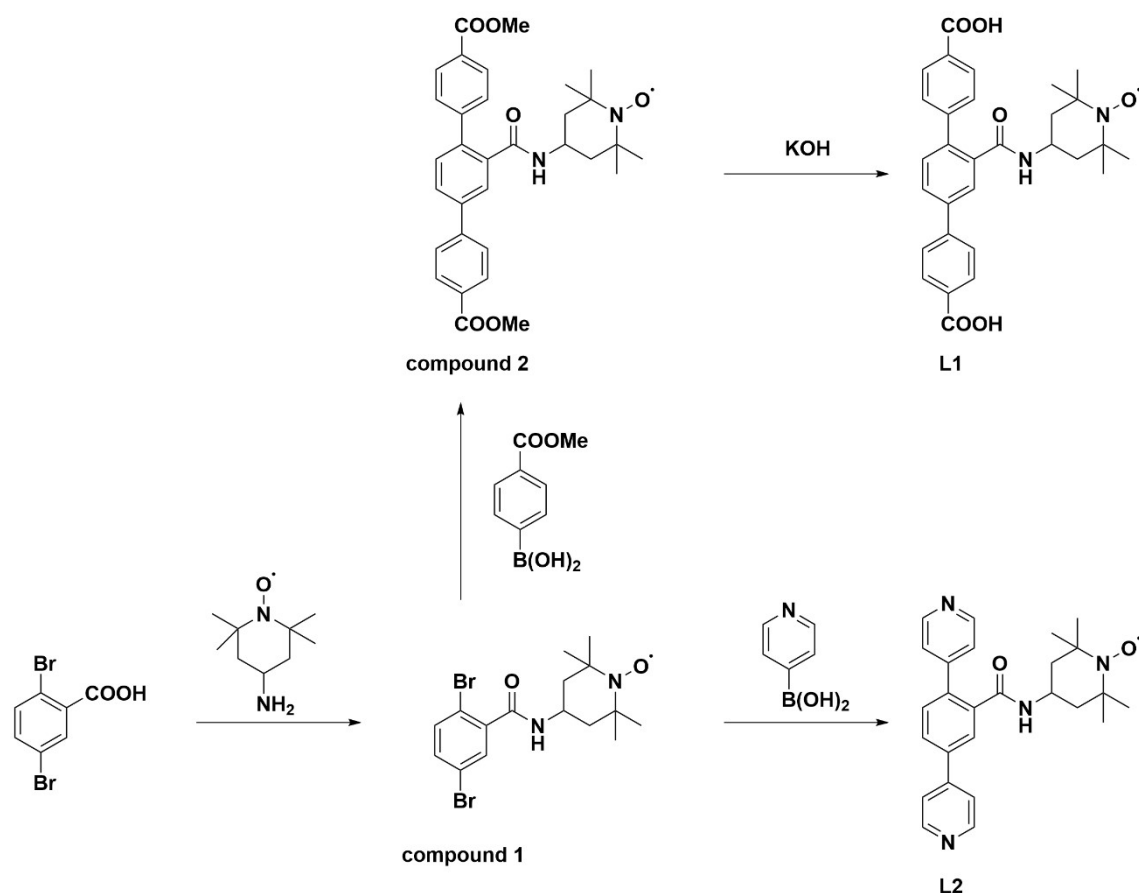
Cycle reaction

After the first catalytic reaction in CD₃CN, the PCP obtained from centrifugation was washed with CH₃CN (5 mL) three times and 80°C activated under vacuum for 2 h to remove residual CH₃CN. The thermal activated PCP was analyzed by PXRD and then reused as the catalyst for the second cycle aerobic oxidation reaction using CD₃CN as solvent. The catalytic cycle performance was characterized by ¹H NMR on the reaction supernatant solution.

Kinetic reaction

To a Schlenk tube containing CD₃CN (1.5 mL) was added PCP crystals (5 mol% equiv. catalyst), alcohol (0.1 mmol) and tert-butyl nitrite (0.02 mmol, 2.06 mg). The tube was sealed and connected to an O₂ balloon. The reaction mixture was heated at 35°C for a certain time, and the supernatant solution was collected by centrifugation for ¹H NMR analysis.

Ligand synthesis



Compound 1. To a 100 mL, two-necked round-bottomed flask was added 2,5-dibromobenzoic acid (2.0 g, 7.14 mmol), anhydrous DCM (25 mL, 0.3M), oxalyl chloride (1g, 7.85 mmol, 1.1eq) and catalytic amount DMF (3 drops). The solution reacted at room temperature for 2h and cooled down to 0°C in the ice bath. A 30mL anhydrous DCM solution containing 4-amino-2,2,6,6-tetramethylpiperidine 1-oxyl (1.1 eq) and Et₃N (4 mL) was added dropwise at 0°C using a constant pressure dropping funnel. The reaction was processed at room temperature under an N₂ atmosphere for another 12 h. The organic solvent was evaporated, and the product was extracted with dichloromethane three times. The combined organic layer was washed with water and brine and dried over MgSO₄. The extract was filtered off, evaporated, and the crude mixture was purified with silica gel chromatography (eluent: hexane/EA = 2/1). The combined solution was evaporated to give **1** orange-red crystal (2.7g, 87% yield).

Compound 2. The stirred solution of **1** (1.73 g, 4 mmol), 4-(methoxycarbonyl) phenylboronic acid (1.80 g, 10 mmol, 25 eq), Pd(dba)₂ (37 mg, 0.01 mmol) Pcy₃ (33 mg, 0.03 mmol) and K₃PO₄ (2.54 g, 20 mmol) in 40 mL of 1,4-dioxane and 10 mL of water was heated to 110°C under nitrogen atmosphere. Stirring was continued for 24h; the mixture was cooled to room temperature. Water was added, and organic compounds were extracted with ethyl acetate three times. The combined organic layer was purified with silica gel chromatography (eluent: hexane/EA = 1/2), giving **2** as a pink powder (1.5 g, 72% yield).

TPDC-TEMPO (ligand L1)

45 mL 4% KOH aqueous solution was added into 45 mL THF solution of compound **2** (1.5 g). The mixture was stirred at room temperature for 5h. The reaction mixture turned from two separative phases to an orange-yellow homogeneous solution. Diluted the orange solution with 50 mL water and washed it with Et₂O (15 mL) 3 times. The aqueous layer was collected and acidified by diluted HCl to pH = 1. The pink precipitate was isolated by centrifugation and collected after H₂O wash with a 90% yield.

To characterize L1 by NMR, the as-synthesized pink precipitate (515 mg, 1 mmol) was dissolved in 4% NaOH aqueous solution (10 mL) and mixed with 0.4 M L-ascorbate aqueous solution (5 mL). The solution was stirred at room temperature for 2h and acidified by diluted HCl. The obtained off-white precipitate was filtered out, washed by H₂O and MeOH, dried under vacuum and analyzed by ¹H NMR. ¹H NMR (DMSO-*d*₆, 400 MHz): δ=13.02 (s, 2H, -COOH), 8.04-8.09(d, 2H, Ar H), 7.97-8.02 (d, 2H, Ar H), 7.88-7.94(m, 3H, Ar H), 7.78 (s, 1H, Ar H), 7.52-7.61 (dd, 3H, Ar H), 4.09 (s, 1H, CH), 1.77(s, 4H, CH₂) and 1.23(s, 12 H, CH₃).

DPyB-TEMPO (Ligand L2)

The stirred solution of **1** (1.73 g, 4 mmol), 4-pyridine boronic acid (1.23 g, 10 mmol, 25 eq), Pd(dba)₂ (37 mg, 0.01 mmol) Pcy₃ (33 mg, 0.03 mmol) and K₃PO₄ (2.54 g, 20 mmol) in 40 mL of 1,4-dioxane and 10 mL of water was heated to 110°C under nitrogen atmosphere. Stirring was continued for 24h; the mixture was cooled to room temperature. Water was added, and organic compounds were extracted with ethyl acetate three times. The combined organic layer was purified with silica gel chromatography (eluent: EA/MeOH = 100/1), giving **L2** a pink powder (1.4 g, 83% yield).

To characterize L2 by NMR, the as-synthesized pink precipitate (429 mg, 1 mmol) was dispersed in a 0.4 M L-ascorbate aqueous solution (10 mL). The pink suspension turned off-white after stirring at room temperature for 2h. Filtered the white solid and washed it with water (10 mL). The solid was further washed with 10 mL acetone, dried under vacuum, and analyzed by ¹H NMR. ¹H NMR (DMSO-*d*₆, 400 MHz): δ=8.68 (s, 2H, Ar H), 8.62 (s, 2H, Ar H), 8.23-8.25 (d, 1H, Ar H), 7.98-8.00(d, 1H, Ar H), 7.87 (s, 1H, Ar H), 7.83 (s, 2H, Ar H), 7.60-7.62 (d, 1H, Ar H), 7.43 (s, 2H, Ar H), 7.13 (s, 1H, OH), 4.0 (d, 1H, CH), 1.59-1.61 (d, 2H, CH₂), 1.22-1.27 (t, 2H, CH₂), 1.04-1.05(12 H, CH₃).

DT-PCP. A MeOH (2 mL) solution of zinc nitrate hexahydrate (15 mg, 0.05 mmol) and L2 (10.7 mg, 0.025 mmol) and a DMF (1 mL) solution of L1 (25.8 mg, 0.05 mmol) was mixed in a 5 mL vial). The small vial was sealed by cap and heated at 60 °C for two days. Cubic shape single crystals were isolated from the mother liquid by dumping to give an isolation yield of 84%. The as-synthesized crystals were washed with DMF three times and stored at room temperature in sealed vials. DT-PCP-ACN/acetone/DCM/toluene single crystals were obtained by the solvent exchange of DT-PCP-DMF single crystal by soaking in the corresponding solvents. DT-PCP single crystals were immersed in the fresh solvent at room temperature for more than one week. The solvent was replaced every 12 h to facilitate thorough exchange.

DT-PCP-guest-free microcrystalline powders were formed by DT-PCP-DCM thermal activation at 80°C for 12 h. Specifically, DT-PCP-DMF single crystal was immersed in DCM for solvent exchange. The solvent exchange was processed under stirring, and fresh DCM was replaced every 4-6 h. 24 h later, PCP was collected by filtration and activated in vacuum at 80°C for 12 h. The complete solvent exchange from DMF to DCM was confirmed by NMR analysis of digested PCP (Figure S7). The microcrystalline powder sample was used for the catalytic investigation without grinding. The particle size ranges from 5 to 25 μm according to SEM in Figure S5.

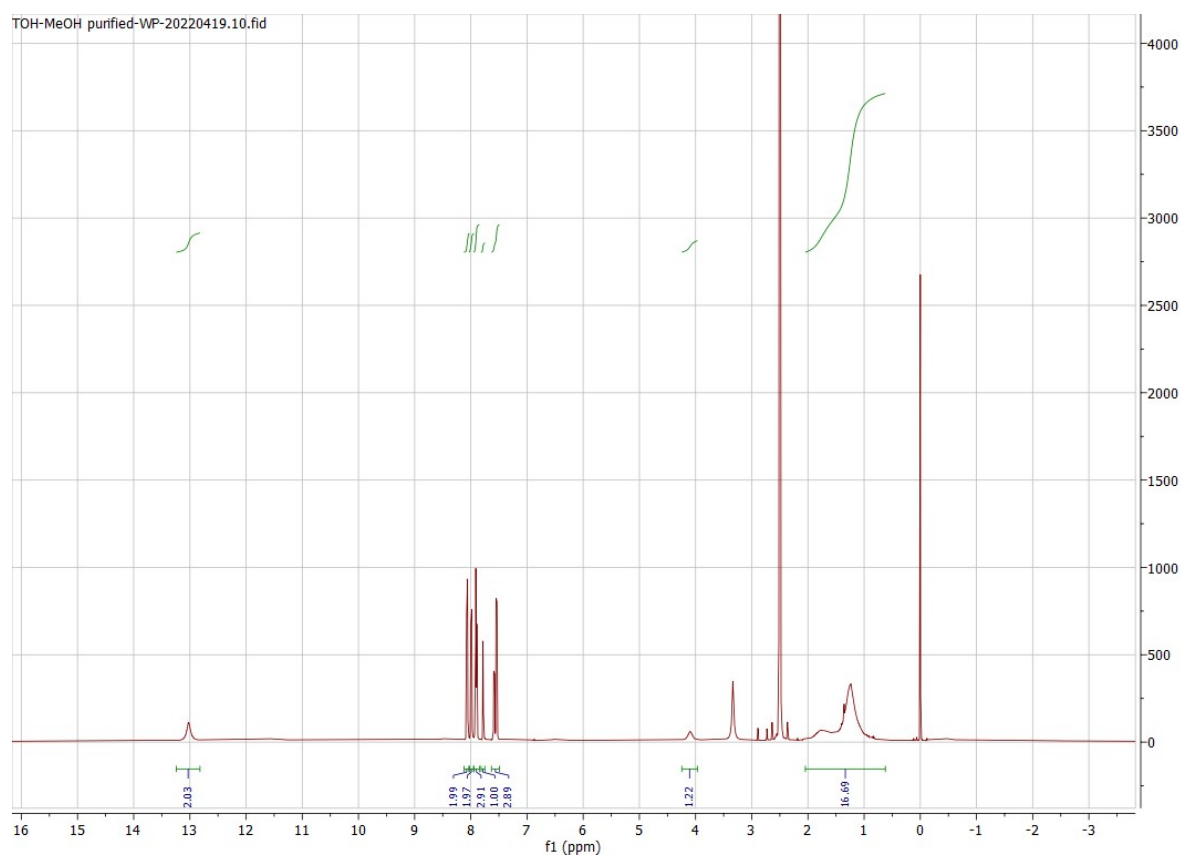


Figure S1. NMR spectrum of ligand TPDC-TEMPO (L1), whose radical is quenched by L-ascorbate.

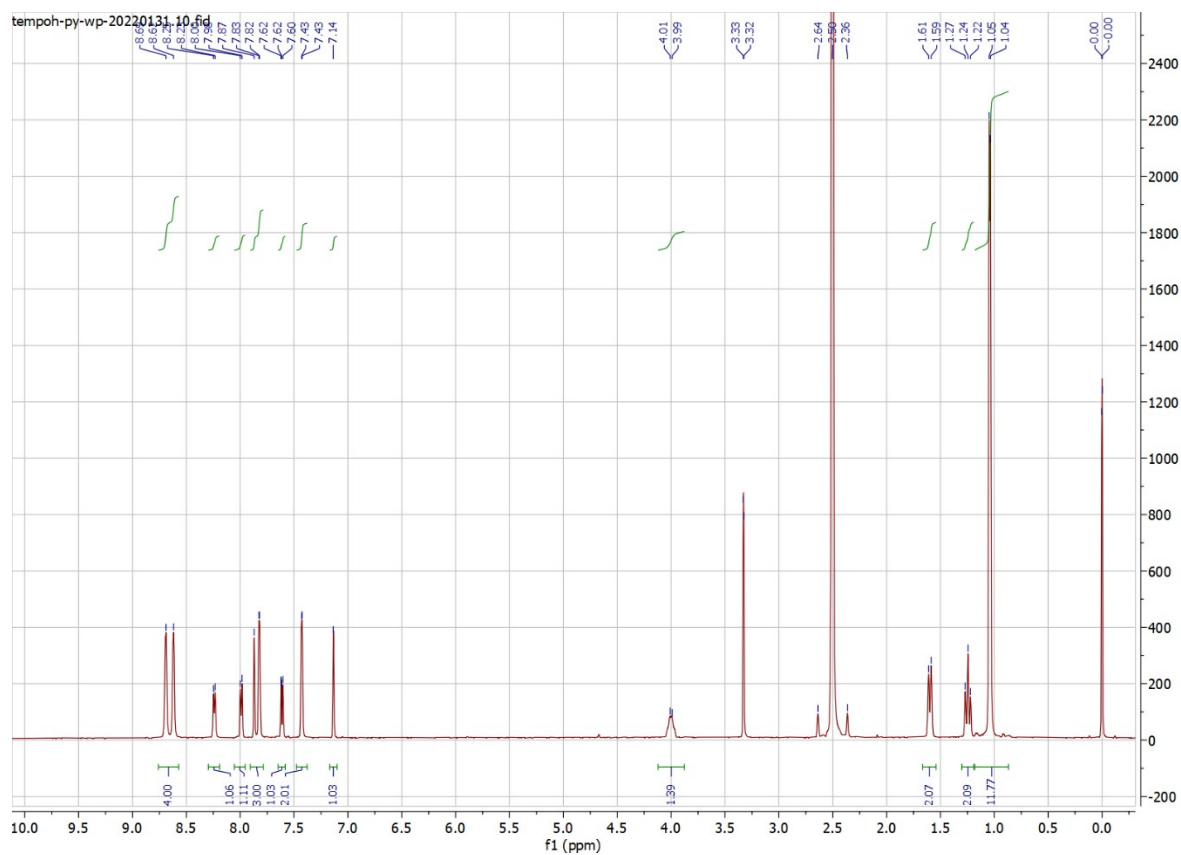


Figure S2. NMR spectrum of ligand DPyB-TEMPO (L2), whose radical is quenched by L-ascorbate.

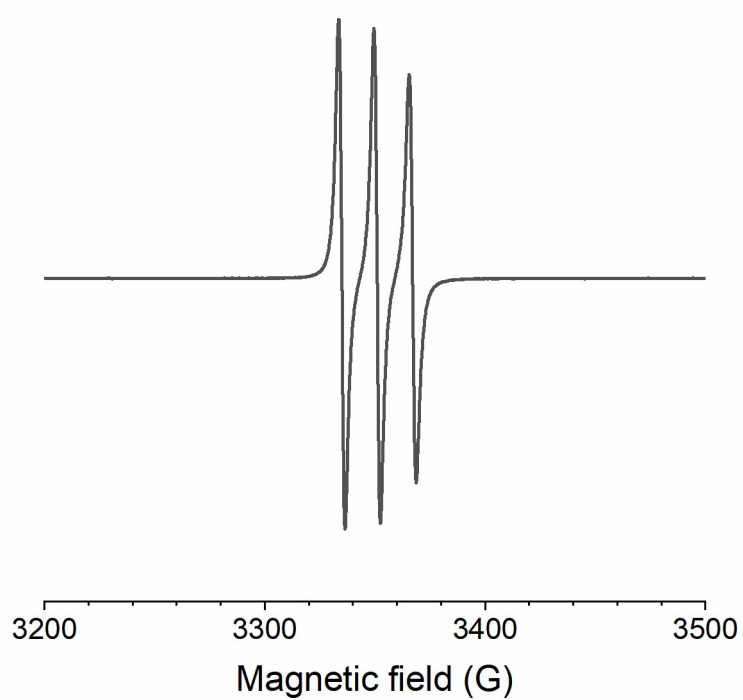


Figure S3. The electron spin resonance (ESR) spectrum of ligand TPDC-TEMPO in MeOH.

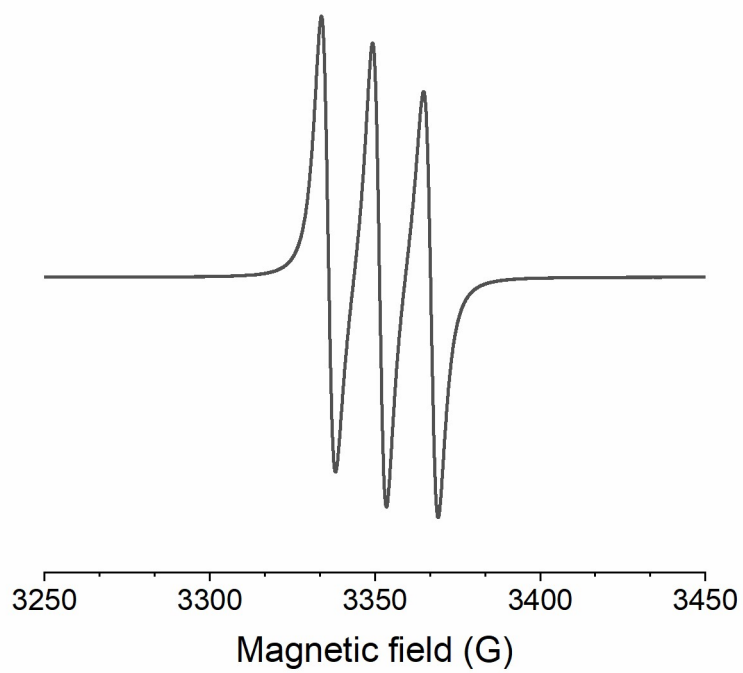


Figure S4. The electron spin resonance (ESR) spectrum of ligand DPyB-TEMPO in MeOH.

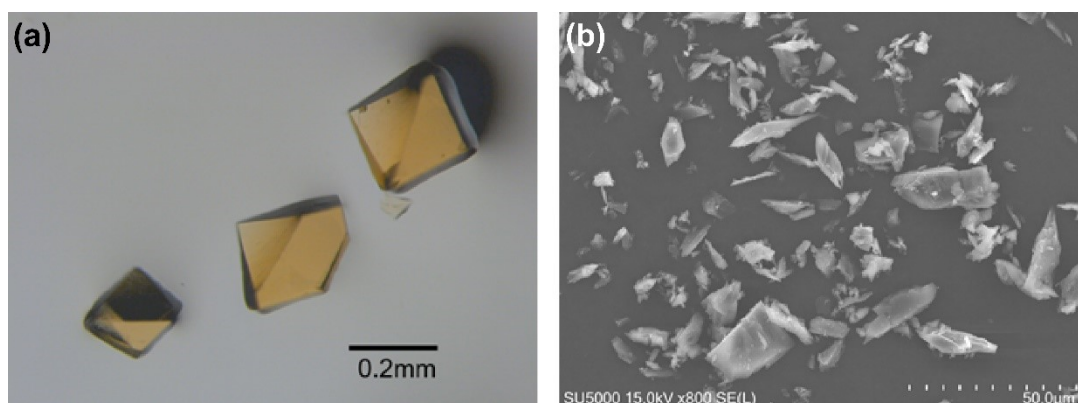


Figure S5. (a) The photo of as-synthesized DT-PCP in DMF. (b) The SEM image of DT-PCP-guest-free used as the aerobic oxidation catalyst.

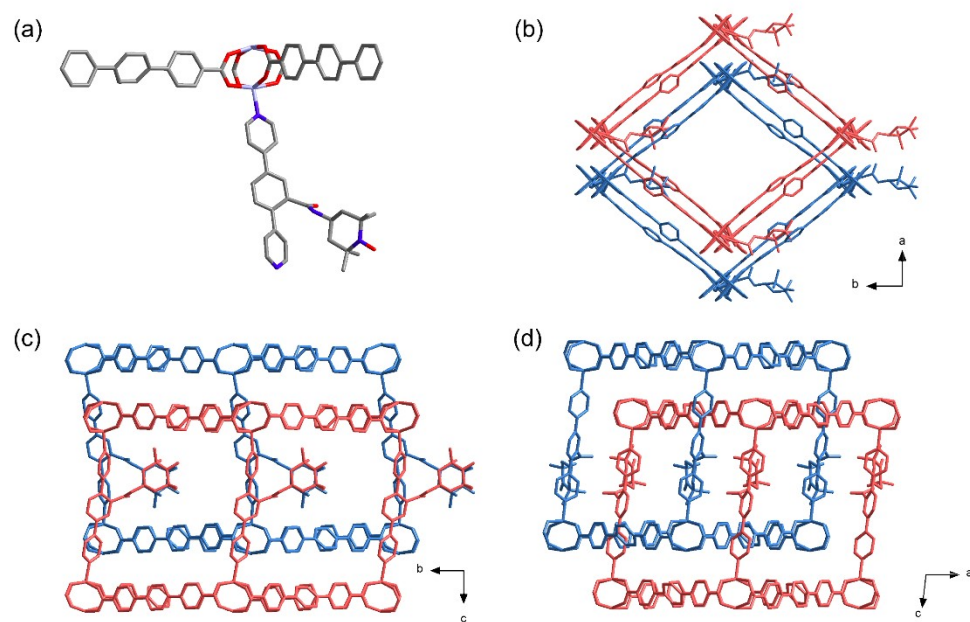


Figure S6. Structure of DT-PCP-DMF.

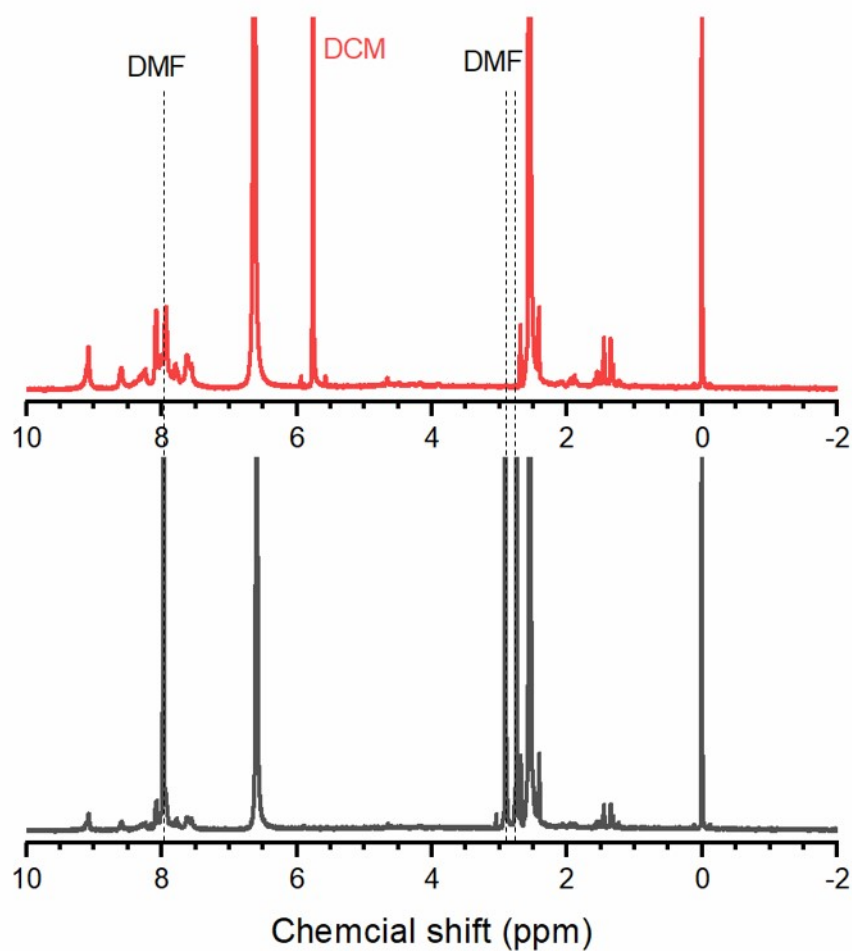


Figure S7. NMR spectra of deuterium chloride digested DT-PCP-DMF before (black) and after (red) DCM exchange. The missing DMF peak identifies the complete exchange.

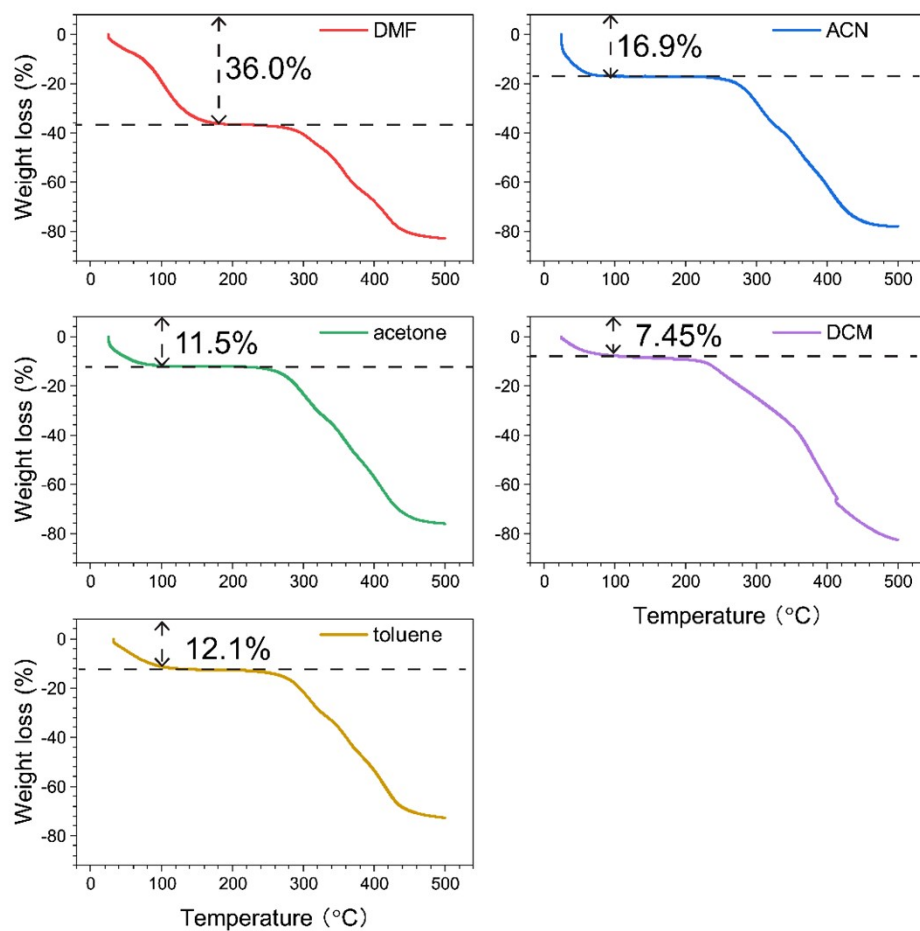


Figure S8. TGA profile of DT-PCP loading different solvents.

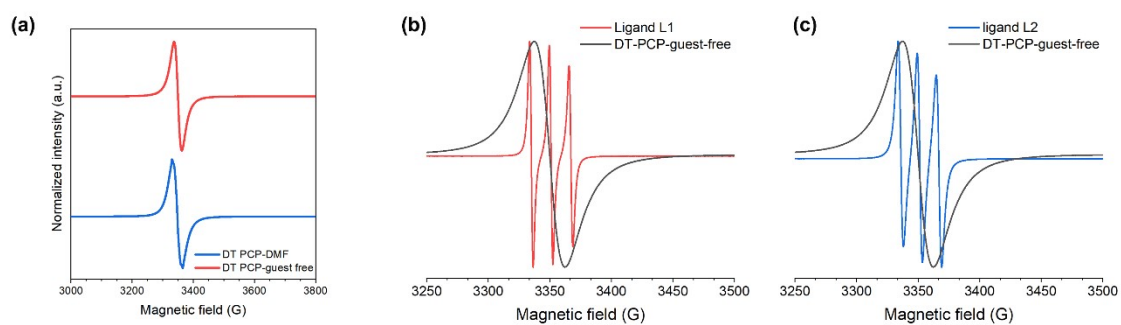


Figure S9. EPR spectrum comparison between DT-PCP-guest-free and ligand.

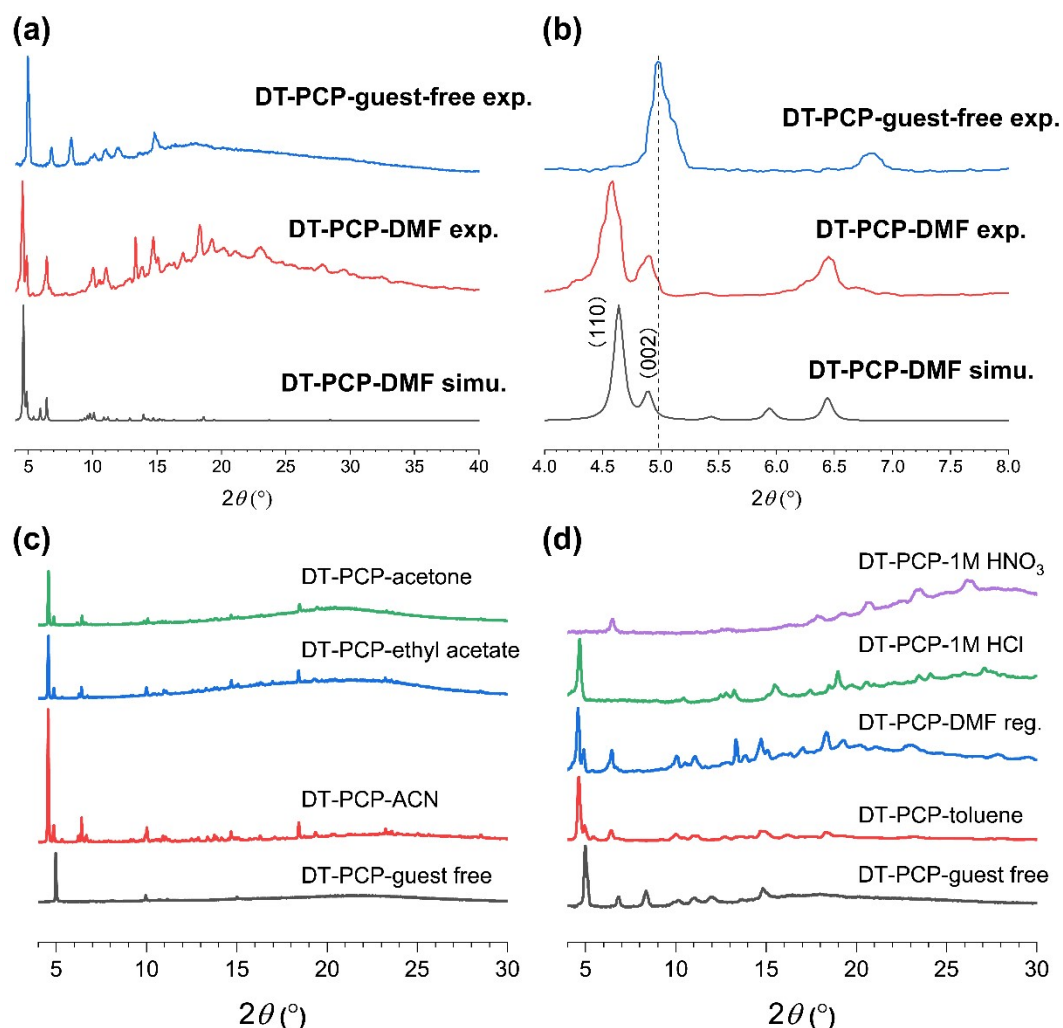


Figure S10. DT PCP PXRD patterns. After guest removal by solvent exchange and thermal activation, the guest-free sample displayed a pattern different from the as-synthesized one. As emphasized in figure (b), the first peak of the guest-free sample shifts to a higher degree. For stability test, guest-free PCP powder was dispersed into organic solvents/ base/acid and kept the mixtures stirring at room temperature. After 24 h, PCPs with organic solvents were sealed in $\phi = 1.0$ mm glass capillary for PXRD measurement (c). PCPs immersed in toluene, DMF and acid were directly isolated by filtration and subjected to PXRD measurement (d). DT-PCP decomposed in 1M NaOH after 24 h stirring at room temperature, leaving no solid available for PXRD analysis.

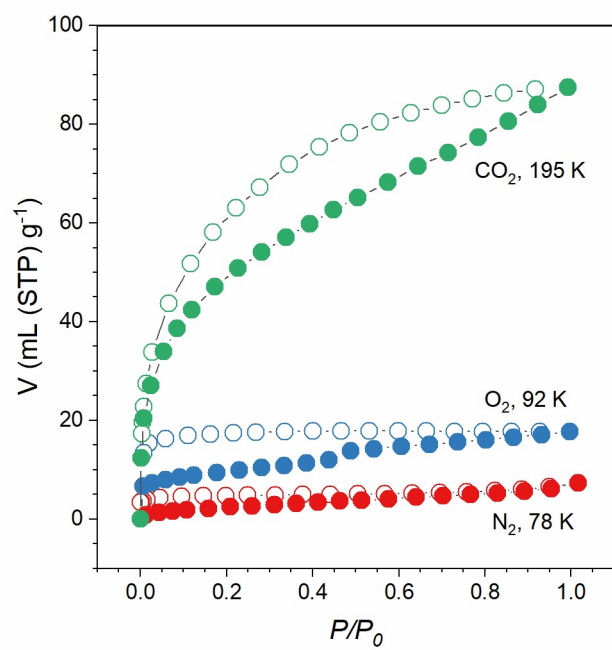


Figure S11. DT-PCP gas adsorption isotherms.

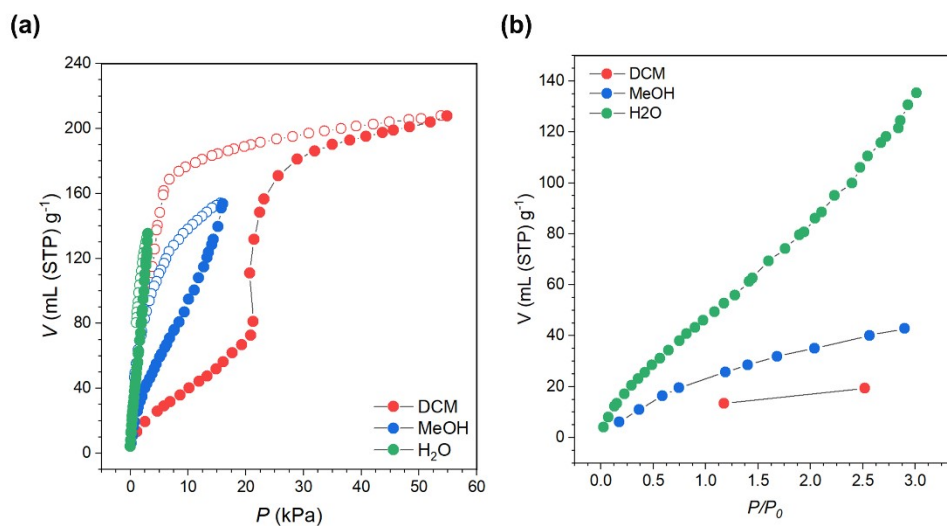


Figure S12. DT-PCP vapor adsorption in the low-pressure range.

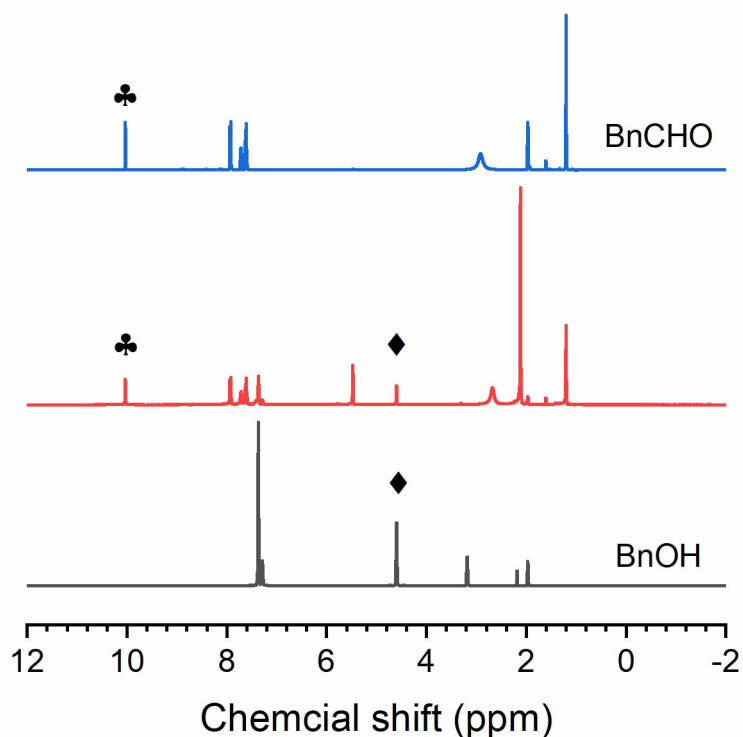


Figure S13. leak check by using solution after 1st catalytic cycle. Fresh reactants were added into the solution isolated from 1st catalytic cycle and reacted at 35°C. After 24h, the reaction solution was isolated and analyzed by NMR (red line). The marks refer to the representative peaks belonging to BnOH and BnCHO, representatively. Without DT-PCP, after 24h, the reactant remains in the reaction system, confirming the system's heterogeneous catalytic nature.

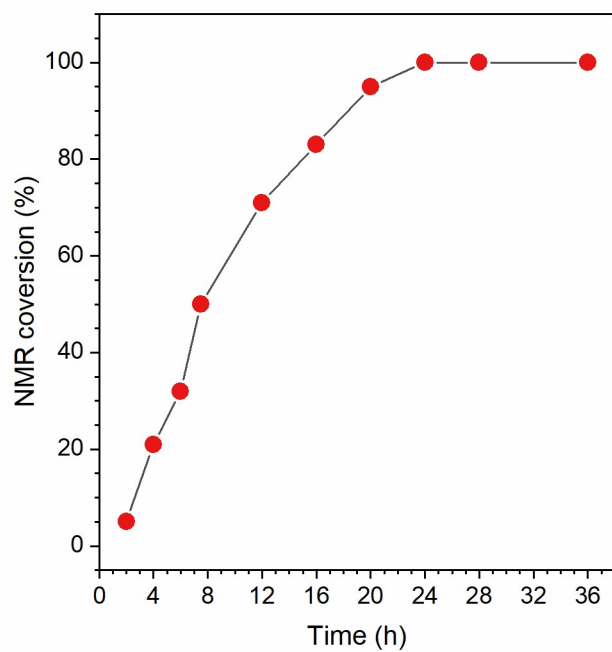


Figure S14. Kinetic study of BnOH oxidation by DT-PCP in CH_3CN at 35°C . DT-PCP TOF in ACN is $4.1 \times 10^{-4} \text{ s}^{-1}$.

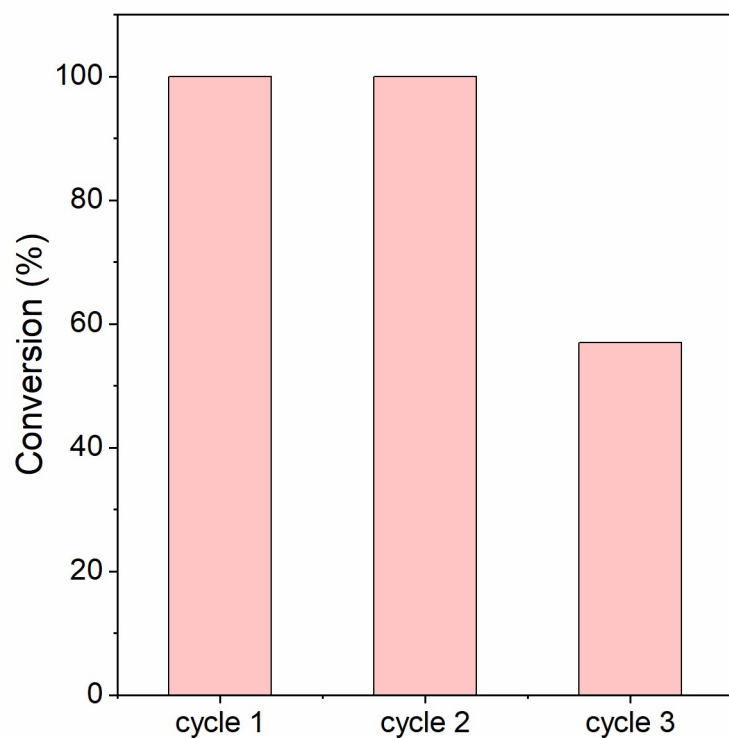


Figure S15. DT-PCP cycle performance for BnOH aerobic oxidation at 35°C. We attribute the decay in the catalytic activity after the second cycle to the sample damage resulting from corrosive byproducts. According to the proposed catalytic mechanism of the TEMPO-based catalyst with the existence of tert-Butyl nitrite (TBN) and O₂, NO_x and H₂O are formed as the byproduct during the reaction process (*ref.* Q. Cao *et al.*, *Chem. Commun.*, 2014, **50**, 4524-4543), which eventually produce HNO₃. According to the chemical stability test, DT-PCP crystallinity decayed severely in the appearance of HNO₃ (Figure S10). Thus, we assume the NO_x and H₂O damaged DT-PCP crystalline structure, leading to the decay of catalytic activity.

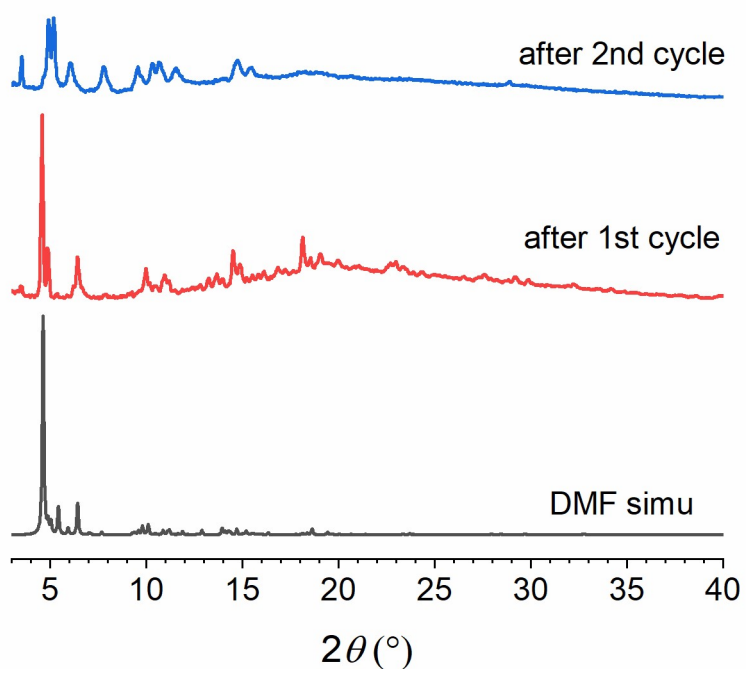


Figure S16. DT-PCP PXRD after cycle catalysis at 35°C.

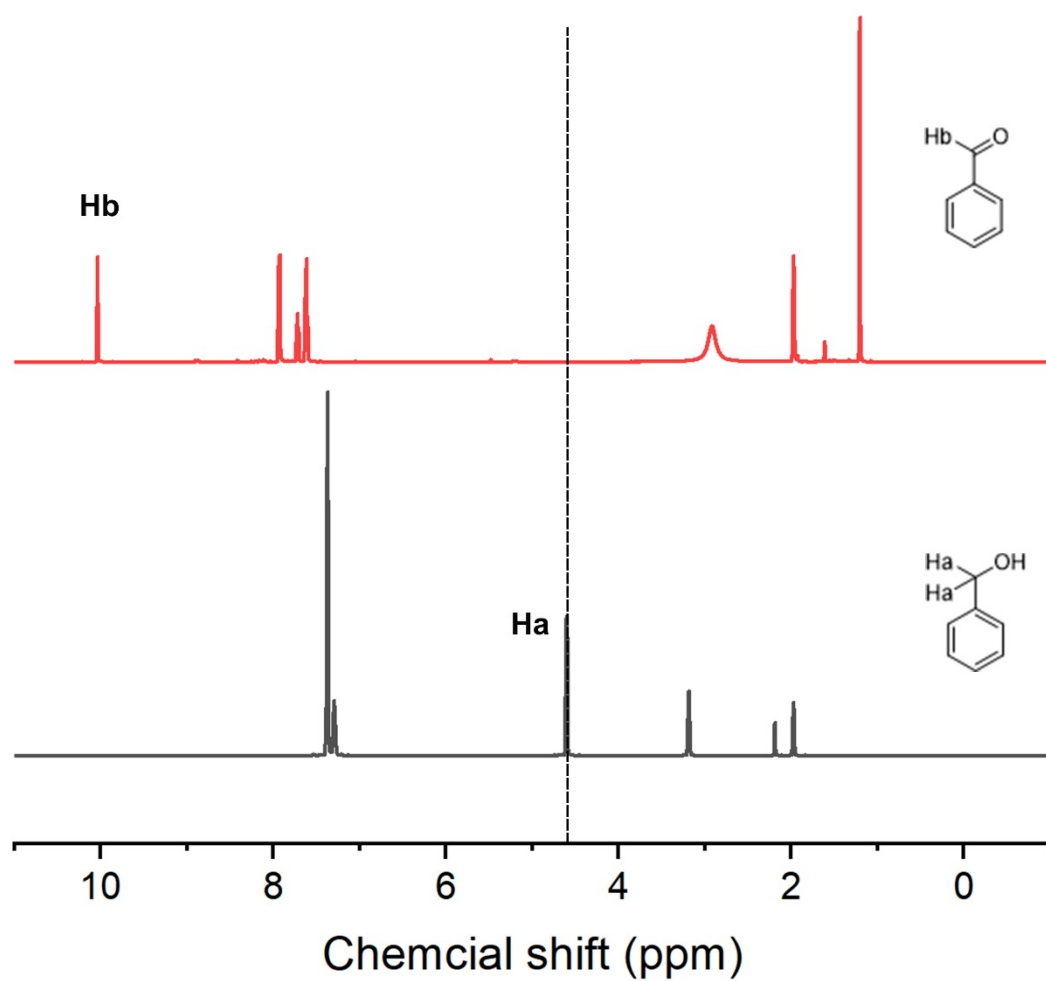


Figure S17. NMR spectra analysis on substrate 1 aerobic oxidation in CD_3CN catalyzed by DT-PCP. At 35°C , substrate 1 (0.1 mmol) reacted in 1.5 mL CD_3CN in the appearance of tert-butyl nitrite (0.02 mmol) for 24 h under O_2 atmosphere.

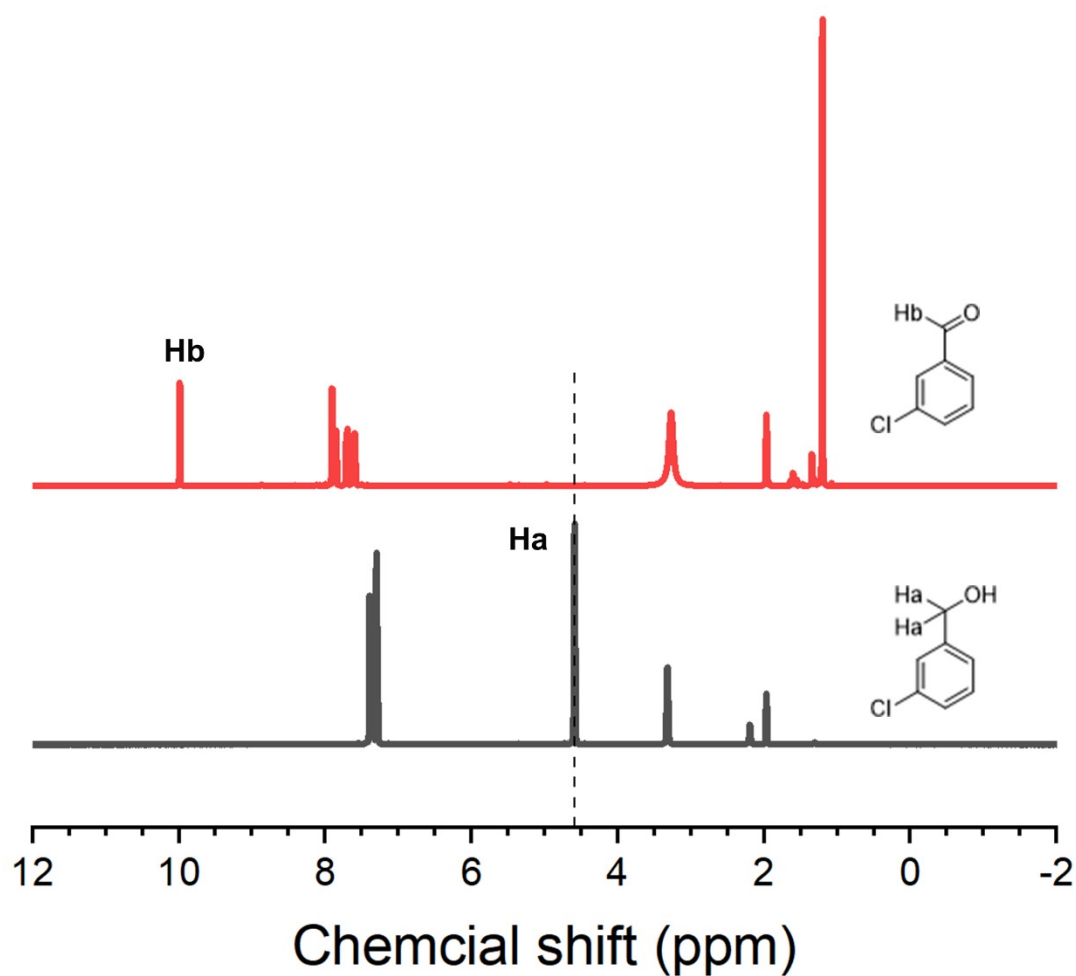


Figure S18. NMR spectra analysis on substrate 2 aerobic oxidation in CD₃CN catalyzed by DT-PCP. At 35°C, substrate 2 (0.1 mmol) reacted in 1.5 mL CD₃CN in the appearance of tert-butyl nitrite (0.02 mmol) for 24 h under O₂ atmosphere.

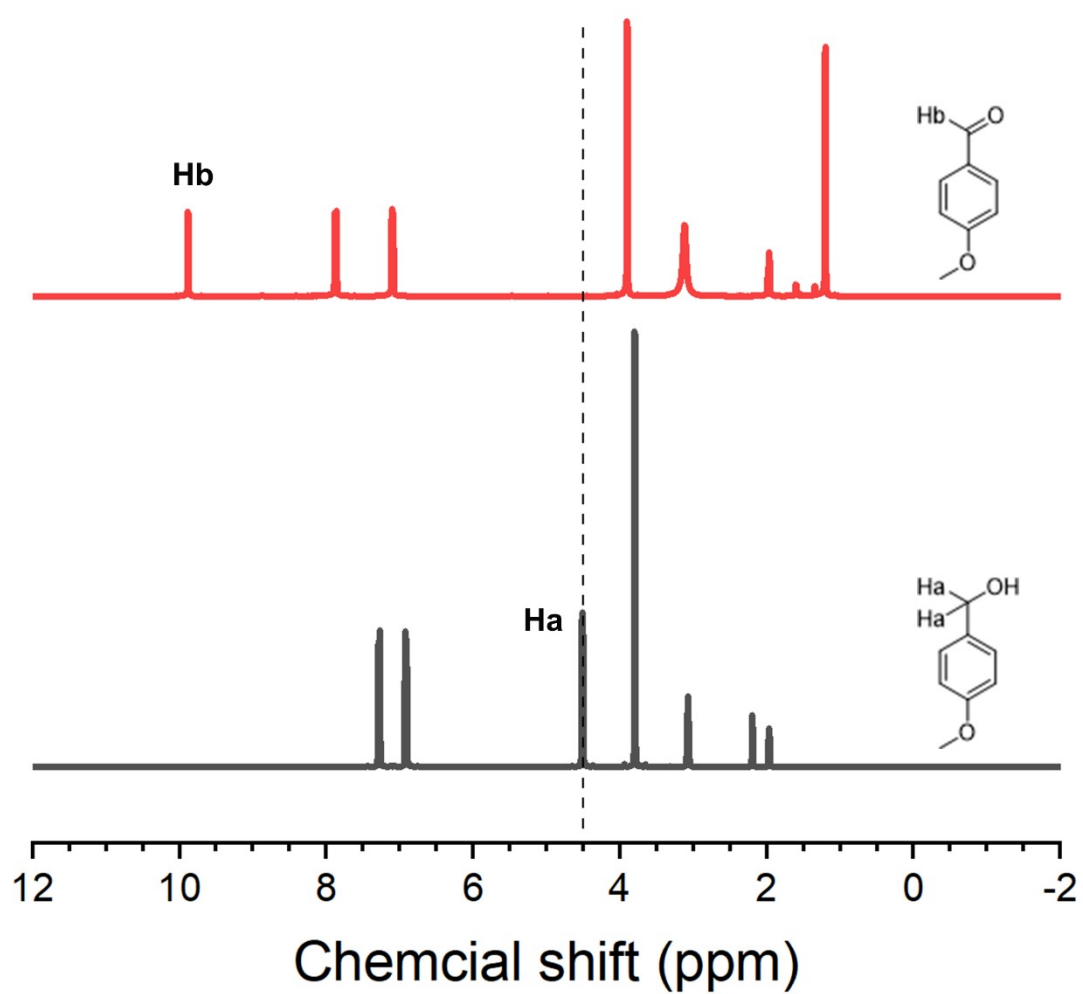


Figure S19. NMR spectra analysis on substrate 3 aerobic oxidation in CD_3CN catalyzed by DT-PCP. At 35°C , substrate 3 (0.1 mmol) reacted in 1.5 mL CD_3CN in the appearance of tert-butyl nitrite (0.02 mmol) for 24 h under O_2 atmosphere.

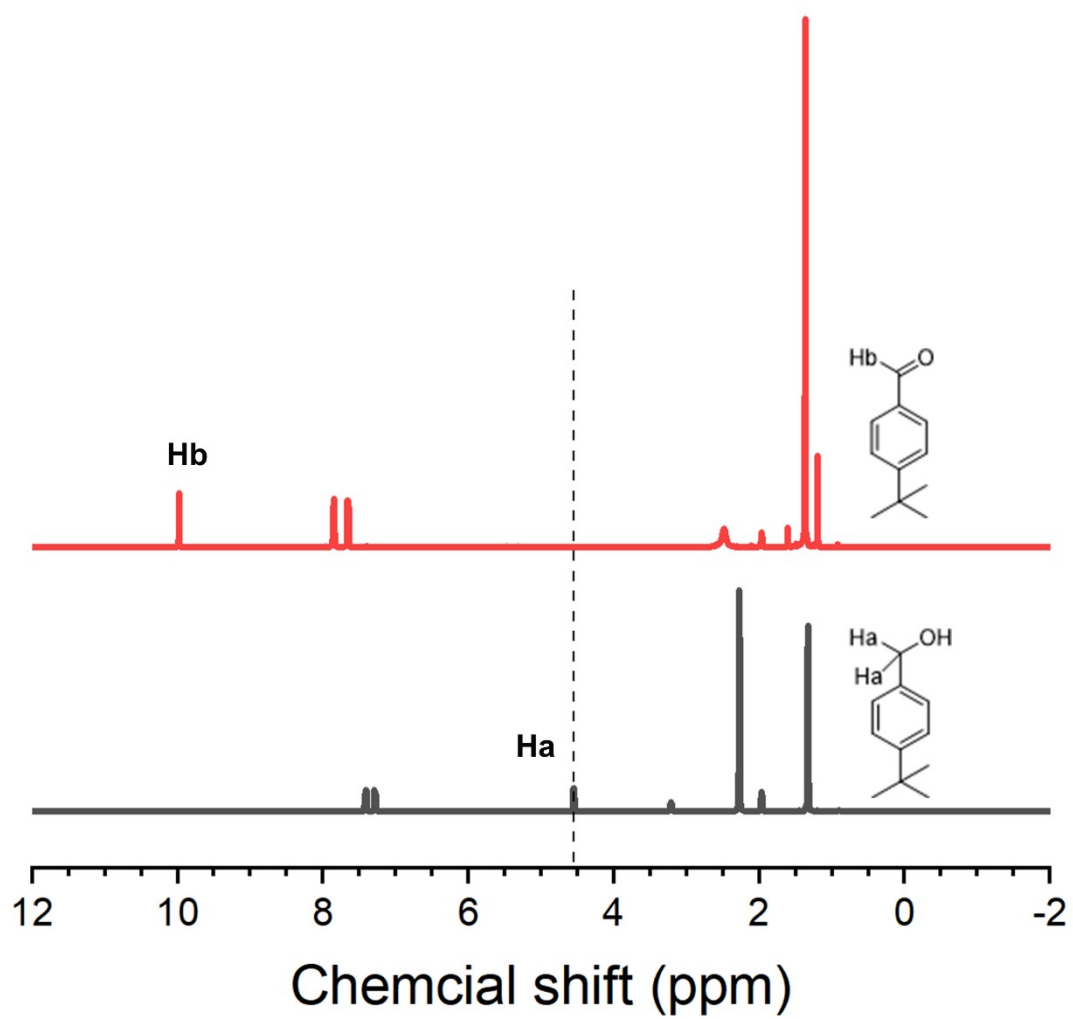


Figure S20. NMR spectra analysis on substrate 4 aerobic oxidation in CD_3CN catalyzed by DT-PCP. At 35°C , substrate 4 (0.1 mmol) reacted in 1.5 mL CD_3CN in the appearance of tert-butyl nitrite (0.02 mmol) for 24 h under O_2 atmosphere.

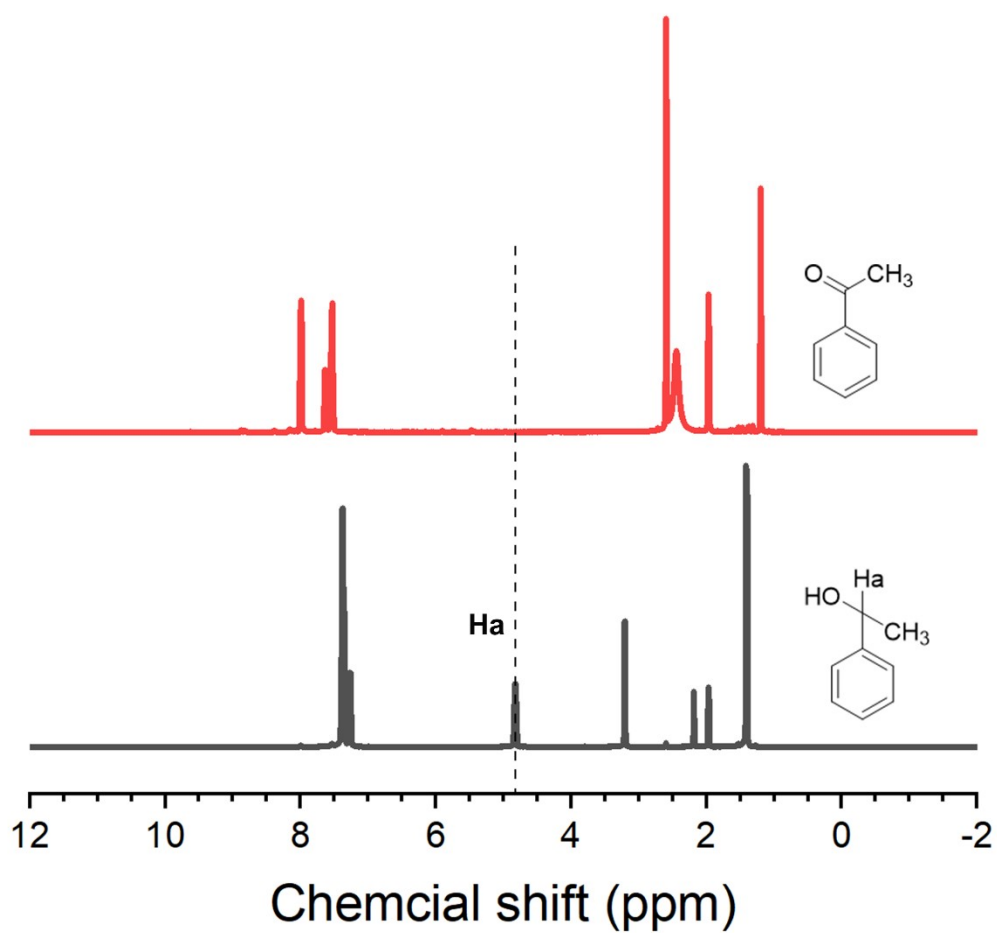


Figure S21. NMR spectra analysis on substrate 5 aerobic oxidation in CD_3CN catalyzed by DT-PCP. At 35°C , substrate 5 (0.1 mmol) reacted in 1.5 mL CD_3CN in the appearance of tert-butyl nitrite (0.02 mmol) for 24 h under O_2 atmosphere.

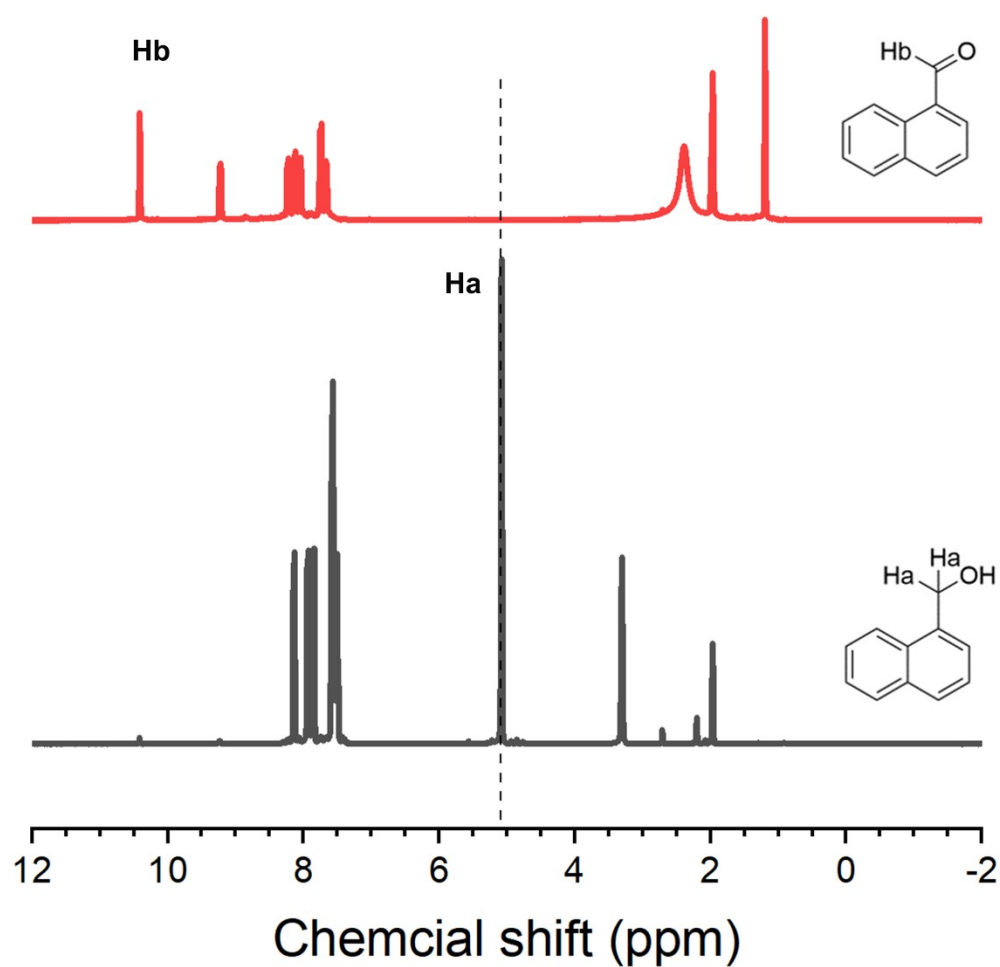


Figure S22. NMR spectra analysis on substrate 6 aerobic oxidation in CD_3CN catalyzed by DT-PCP. At 35°C , substrate 6 (0.1 mmol) reacted in 1.5 mL CD_3CN in the appearance of tert-butyl nitrite (0.02 mmol) for 24 h under O_2 atmosphere.

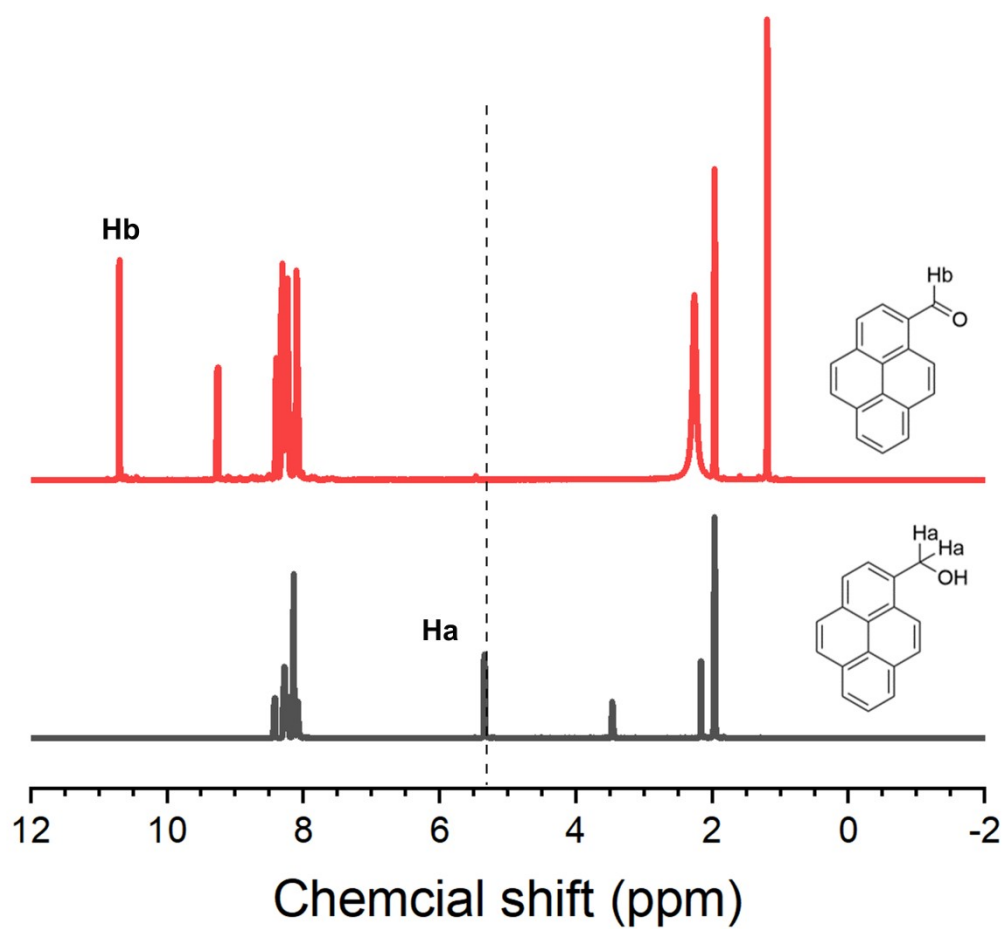


Figure S23. NMR spectra analysis on substrate 7 aerobic oxidation in CD_3CN catalyzed by DT-PCP. At 35°C , substrate 1 (0.1 mmol) reacted in 1.5 mL CD_3CN in the appearance of tert-butyl nitrite (0.02 mmol) for 24 h under O_2 atmosphere.

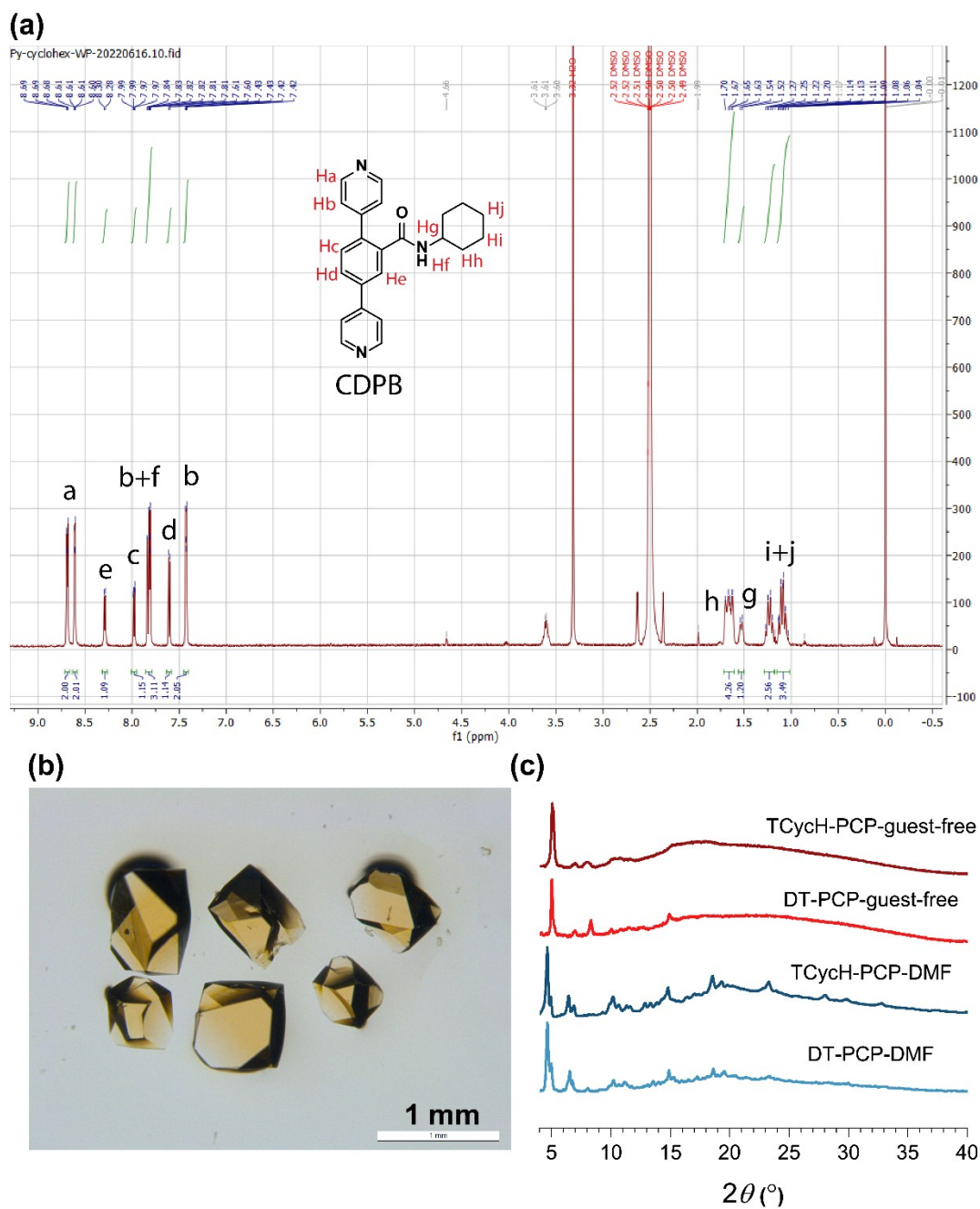


Figure S24. TCycH-PCP with diluted TEMPO-density. (a) NMR of ligand CDPB whose cyclohexane substituent is spatially similar to TEMPO. (b) the crystal photo of as-synthesized TCycH-PCP-DMF. (c) PXRD patterns of TCycH-PCP-DMF and TCycH-PCP-guest-free are identical to those of DT-PCP-DMF and DT-PCP-guest-free.

Crystal size effect

To test the crystal size effect on catalytic efficiency, we performed the catalytic reaction using the large single crystals of DT-PCP. Specifically, we activated DT-PCP-DCM single crystals at room temperature. DT-PCP-DCM single crystals were activated at room temperature. The guest-free PCP maintained the original crystals' morphology and size ($\sim 500\ \mu\text{m}$), although many cracks were observed on their crystal surfaces. These crystals were then used as the catalyst at 35°C without stirring. NMR spectrum reveals that the conversion for BnOH was 46% when the single crystal was used as the catalyst. This value is much smaller than powder DT-PCP ($> 99\%$) under similar reaction conditions with the same reaction time. Thus, we confirm a crystal size effect for DT-PCP catalytic efficiency, probably due to the limitation of substrate diffusion in the large crystals.

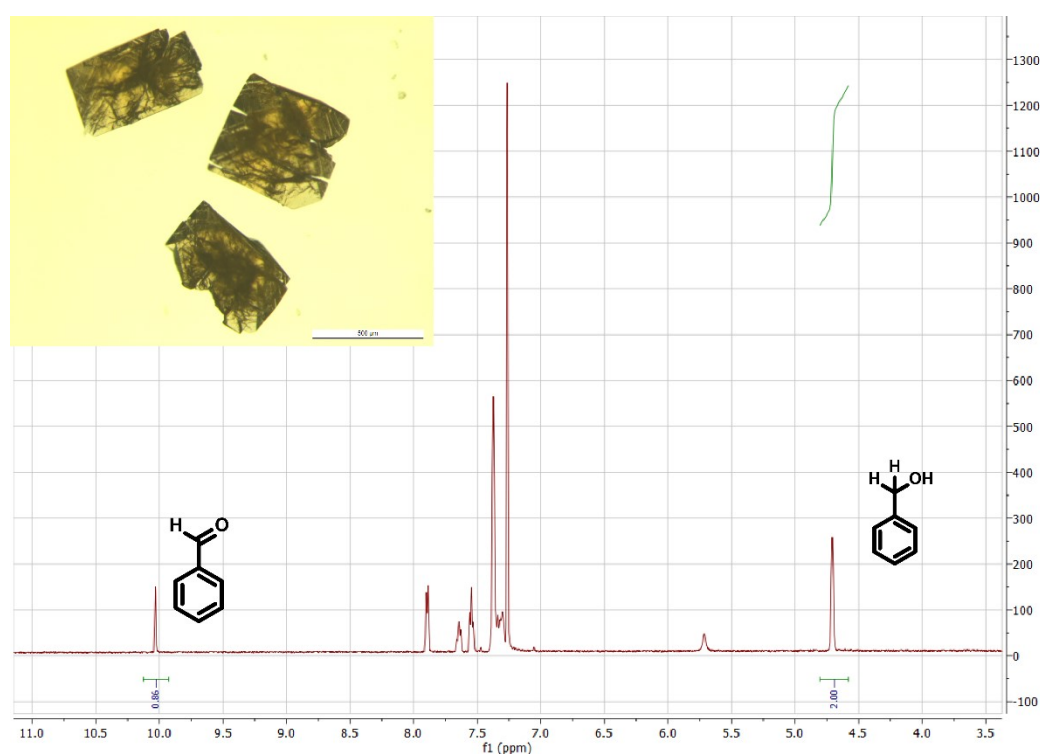
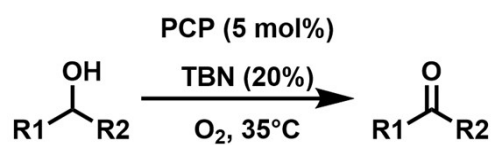


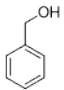
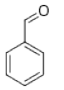
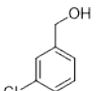
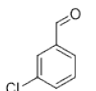
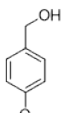
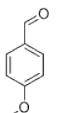
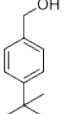
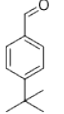
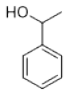
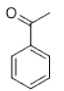
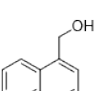
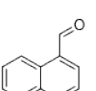
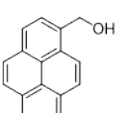
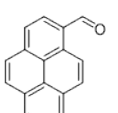
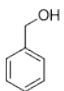
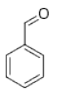
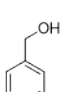
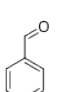
Figure S25. NMR spectra analysis on BnOH aerobic oxidation in ACN catalyzed by single-crystal DT-PCP. At 35°C , BnOH (0.1 mmol) reacted in 1.5 mL ACN in the appearance of tert-butyl nitrite (0.02 mmol) for 24 h under an O_2 atmosphere.

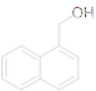
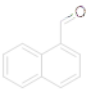
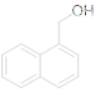
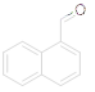
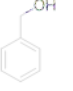
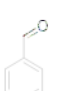
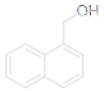
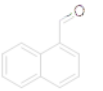
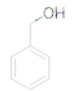
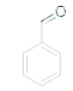
Table S1. Crystallographic parameters for PCPs with different solvent guest species.

PCP	DT-PCP-DMF	DT-PCP-DCM	DT-PCP-Acetone	DT-PCP-Acetonitrile	DT-PCP-Toluene
T (K)	100	100	100	100	100
λ (Å)	0.71073	0.41250	0.41280	0.41280	0.71073
Crystal system	Monoclinic	Monoclinic	Monoclinic	Monoclinic	Monoclinic
Space group	$C 2/c$ (15)	$C 2/c$ (15)	$C 2/c$ (15)	$C 2/c$ (15)	$C 2/c$ (15)
a (Å)	24.939(1)	26.173(13)	26.112(11)	26.235(1)	26.1988(9)
b (Å)	29.750(1)	28.219(14)	28.570(17)	28.668(1)	28.6120(9)
c (Å)	36.332(1)	35.844(18)	36.062(14)	36.176(1)	36.1248(10)
α (°)	90	90	90	90	90
β (°)	96.591(3)	104.199(7)	102.016(10)	101.005(7)	103.038(3)
γ (°)	90	90	90	90	90
V (Å ³)	26778(2)	25665(22)	26314(22)	26707(2)	26381(2)
Crystal dimension(mm ³)	0.15×0.10 ×0.04	0.15×0.15 ×0.15	0.10×0.10 ×0.10	0.02×0.02 ×0.02	0.10×0.05 ×0.03
R_{int}	0.0772	0.1095	0.0727	0.0994	0.0509
Goodness-of-Fit	1.043	1.141	0.972	1.054	1.109
R_1 ($I > 2.0\sigma(I)$)	0.1187	0.1146	0.0904	0.0997	0.0934
wR_2 (all data)	0.3887	0.3471	0.2888	0.3187	0.3228
CCDC deposition number	2172787	2172786	2172789	2172785	2172788

Table S2. DT-PCP catalyzed aerobic oxidation of various alcohols.



Entry	PCP	substrate	product	Solvent	time (h)	conversion (%)
1	DT-PCP			ACN	24	>99
2	DT-PCP			ACN	24	>99
3	DT-PCP			ACN	24	>99
4	DT-PCP			ACN	36	>99
5	DT-PCP			ACN	24	>99
6	DT-PCP			ACN	24	>99
7	DT-PCP			ACN	24	>99
8	DT-PCP			Acetone	36	83.7
9	DT-PCP			DCM	36	14.5

10	DT-PCP			Acetone	48	42.5
11	DT-PCP			DCM	48	9.5
12	DT-PCP			Acetone	48	89
						63
13	TCycH-PCP			ACN	36	98